

Nuclear antiferromagnetism in copper: Interplay of $(0, \frac{2}{3}, \frac{2}{3})$ and $(1,0,0)$ order

H. E. Viertiö

Research Institute for Theoretical Physics, University of Helsinki, SF-00170 Helsinki, Finland

A. S. Oja

Low Temperature Laboratory, Helsinki University of Technology, SF-02150 Espoo, Finland

(Received 21 June 1990)

The magnetic phase diagram of nuclear spins in copper, an ideal fcc system, is investigated. The recently observed interplay of the antiferromagnetic $(0, \frac{2}{3}, \frac{2}{3})$ and $(1,0,0)$ order at nanokelvin temperatures is explained by using the concept of permanent spin structures. At low fields, the strongly anisotropic spin interactions stabilize the field-induced $(0, \frac{2}{3}, \frac{2}{3})$ order which coexists with the $(1,0,0)$ order in a single magnetic domain. The spin structure at zero field and at high fields is of the $(1,0,0)$ -type.

Recently, Annala *et al.*¹ reported observation of the $(0, \frac{2}{3}, \frac{2}{3})$ neutron Bragg reflection in the nuclear-spin system of copper at nanokelvin temperatures. Three antiferromagnetic phases were found as a function of the external magnetic field, aligned in the $[01\bar{1}]$ crystalline direction. In low fields, the previously observed² $(1,0,0)$ signal and the novel $(0, \frac{2}{3}, \frac{2}{3})$ reflection are present simultaneously. Around 0.08 mT, only the $(0, \frac{2}{3}, \frac{2}{3})$ reflection was seen, while the order in still higher fields is of the $(1,0,0)$ -type. These observations were quite surprising: The $(0, \frac{2}{3}, \frac{2}{3})$ reflection is not consistent with any previous experimental or theoretical spin structures in an fcc lattice.³

It would be important to find an explanation of the experimental findings. Copper has become a prototype system in extensive theoretical efforts⁴⁻¹³ to understand collective magnetic phenomena on the basis of microscopic spin interactions. As an fcc antiferromagnet the spin system suffers from frustration. Unlike most electronic magnets, nuclear spins in copper are amenable to quantitative predictions: Copper is a pure element with a simple lattice structure, the nuclear spins are well localized and decoupled from the lattice degrees of freedom at low temperatures, and the spin interactions can be calculated from first-principles electronic band structure and wave functions.

In this Rapid Communication the intriguing interplay of the $(0, \frac{2}{3}, \frac{2}{3})$ and $(1,0,0)$ order is explained. By using the concept of *permanent*¹⁴ spin structures, we show that an external-field-induced antiferromagnetic $(0, \frac{2}{3}, \frac{2}{3})$ ordering is stabilized between the zero-field and high-field $(1,0,0)$ phases. The basic ideas are first stated in the framework of the mean-field (MF) theory; the effects of thermal fluctuations are then accounted for by Monte Carlo (MC) simulations. Our theoretical phase diagram explains the observed antiferromagnetic neutron reflections. In low fields the structure is most remarkable: We find that a single magnetic domain displays both $(0, \frac{2}{3}, \frac{2}{3})$ and $(1,0,0)$ order. When the external field is aligned in the $[001]$ direction, we also obtain three phases, in good agreement with the measured field-entropy phase diagram.¹⁵

Nuclear spins in copper interact via the dipolar force

and the conduction-electron-mediated indirect interaction. The latter mainly consists of the isotropic and antiferromagnetic Ruderman-Kittel interaction, which has been calculated from first principles.^{6,7,13} Since the dipolar interaction dominates, the coupling $\mathbf{A}(\mathbf{r}_{ij})$ between spins \mathbf{S}_i and \mathbf{S}_j is strongly anisotropic. A MF analysis leads to the eigenvalue equation^{4,5}

$$\mathbf{A}(\mathbf{k}) \cdot \mathbf{e}_n(\mathbf{k}) = \lambda_n(\mathbf{k}) \mathbf{e}_n(\mathbf{k}), \quad n = 1, 2, 3, \quad (1)$$

where $\lambda_n(\mathbf{k})$ are the eigenvalues and $\mathbf{e}_n(\mathbf{k})$ the eigenvectors of the Fourier sum $\mathbf{A}(\mathbf{k}) = \sum_j \mathbf{A}(\mathbf{r}_{ij}) \exp(-i\mathbf{k} \cdot \mathbf{r}_{ij})$ of the interactions. The ground state is characterized by the ordering vector \mathbf{Q} , found from $\lambda_{\min}(\mathbf{Q}) = \min_{\mathbf{k}, n} \{\lambda_n(\mathbf{k})\}$ if the spin structure $\mathbf{S}_i = \mathbf{S}(\mathbf{Q}) \exp(i\mathbf{Q} \cdot \mathbf{r}_i)$ with $\mathbf{S}(\mathbf{Q}) = \mathbf{e}_{\min}(\mathbf{Q})$ can be chosen permanent,^{5,14} i.e., if the magnitudes of the local fields are independent of the site of the spin. Multi- \mathbf{Q} structures can be constructed by including other vectors belonging to the star of \mathbf{Q} , here denoted by $\langle Q_x, Q_y, Q_z \rangle$.

The ordered spin arrangement in copper has been predicted⁴ to be a type-I antiferromagnet with the ordering vectors $(1,0,0)$, $(0,1,0)$, and $(0,0,1)$, where the prefactor $2\pi/a$ has been dropped. The type-I structure is continuously degenerate in the MF theory,⁴ even in an arbitrary magnetic field.⁵ Quantum⁸⁻¹⁰ and thermal^{11,12} fluctuations lift the degeneracy and, depending on the theoretical model, result in various phase diagrams and spin structures as a function of the external magnetic field. However, all the previous calculations^{8-10,12} for fields in the $[01\bar{1}]$ direction are in serious disagreement with the experimental neutron-diffraction data.^{1,2}

First-principles calculations have shown that in addition to the global minimum of $\lambda_n(\mathbf{k})$ at $\langle 1,0,0 \rangle$ there is a local minimum in the $[110]$ direction,^{6,13} which has been proposed^{9,10} to play a role in ordering. The calculated¹³ $\lambda_{\min}(0, \frac{2}{3}, \frac{2}{3})$ is only 10% larger than $\lambda_{\min}(1,0,0)$: The difference is on the order of the reported 10% uncertainty.

There is a unique eigenvector corresponding to the $(0, \frac{2}{3}, \frac{2}{3})$ order, while for $(1,0,0)$ there are two degenerate eigenvectors, which span an easy plane of anisotropy. An important consequence is that permanent $\langle 1,0,0 \rangle$ structures can be constructed for arbitrary magnetic fields,⁵

whereas permanent $\langle 0, \frac{2}{3}, \frac{2}{3} \rangle$ states exist only for discrete values of the field. An interesting situation occurs if $\lambda_{\min}(0, \frac{2}{3}, \frac{2}{3})$ is slightly lower than $\lambda_{\min}(1,0,0)$. The system then chooses the $\langle 0, \frac{2}{3}, \frac{2}{3} \rangle$ state at fields for which it is permanent; at other fields the system must compromise.

We now consider the limit of degenerate $\langle 0, \frac{2}{3}, \frac{2}{3} \rangle$ and $\langle 1,0,0 \rangle$ order. More precisely,

$$\Delta\lambda \equiv \lambda_{\min}(1,0,0) - \lambda_{\min}(0, \frac{2}{3}, \frac{2}{3}) \rightarrow 0_+.$$

The MF ground state can be found by determining the structure which (i) is permanent and (ii) maximizes the $\langle 0, \frac{2}{3}, \frac{2}{3} \rangle$ order. For the realistic case of positive $\Delta\lambda$ it would be difficult to find the ground state analytically because the energetically favorable $\langle 0, \frac{2}{3}, \frac{2}{3} \rangle$ order tends to stabilize nonpermanent structures. However, we will show that the relevant physics is contained in the solution for $\Delta\lambda \rightarrow 0_+$.

In zero field, there are no permanent spin structures based on the $\langle 0, \frac{2}{3}, \frac{2}{3} \rangle$ order. Therefore, a $\langle 1,0,0 \rangle$ structure is stable as observed;² see Fig. 1(a). In the $[01\bar{1}]$ field direction, that was used in the experiments,^{1,2} we find a permanent structure of the $\langle 0, \frac{2}{3}, \frac{2}{3} \rangle$ order only at $B = B_c/3$, where B_c is the critical field for transition to the paramagnetic state. In this structure two sublattices are oriented parallel to the field and one sublattice antiparallel to it, as illustrated in Fig. 1(c). When $B < B_c/3$, the permanency can be retained if the system develops $\langle 1,0,0 \rangle$ order as well. The MF equation for the ground state is

$$\begin{aligned} \mathbf{S}_i = & (0, d_0, -d_0) + (0, d_1, -d_1) \cos[(0, \frac{2}{3}, \frac{2}{3}) \cdot \mathbf{r}_i] \\ & + (0, d_2, d_2) \cos[(1,0,0) \cdot \mathbf{r}_i] \\ & + (d_3, 0, 0) \cos[(0, 1, 0) \cdot \mathbf{r}_i], \end{aligned} \quad (2)$$

where $-d_1/4 = d_0 = B/(B_c\sqrt{2})$ and $2d_2^2 + d_3^2 = 1 - (3B/B_c)^2$; see Fig. 1(b). When the field is reduced, the $\langle 1,0,0 \rangle$ order grows continuously while the $\langle 0, \frac{2}{3}, \frac{2}{3} \rangle$ component goes to zero at $B = 0$. At fields $B > B_c/3$, no permanent spin arrangement with $\langle 0, \frac{2}{3}, \frac{2}{3} \rangle$ order exists. Therefore, a first-order transition to a $\langle 1,0,0 \rangle$ -type structure takes place at $B = B_c/3$.

The high-field structure shows an extensive degeneracy associated with possible linear combinations of the $\langle 1,0,0 \rangle$ ordering vectors.⁵ Further, in the low-field phase of Eq. (2), the $\langle 1,0,0 \rangle$ order is degenerate. Importantly, however, there is no degeneracy in the $\langle 0, \frac{2}{3}, \frac{2}{3} \rangle$ order: The field

along $[01\bar{1}]$ singles out the two equivalent ordering vectors $\pm(0, \frac{2}{3}, \frac{2}{3})$, in agreement with the experiment.¹

The degeneracy of the MF solution in finite temperatures is lifted by thermal fluctuations. A positive $\Delta\lambda$ removes the degeneracy even in the MF theory. We have studied these effects by MC simulations. For this purpose the dependence of the eigenvalues, $\lambda_{\min}(1,0,0)$ and $\lambda_{\min}(0, \frac{2}{3}, \frac{2}{3})$, on the elements of the interaction matrices $\mathbf{A}(\mathbf{r}_{ij})$ was analyzed. We then constructed model Hamiltonians by slightly varying the calculated¹³ $\mathbf{A}(\mathbf{r}_{ij})$ to produce different $\Delta\lambda$. The interactions were truncated to 140 nearest neighbors. In the simulations the spin structures depended on $\Delta\lambda$, rather than on the detailed form of the Hamiltonian.

Several kinds of MC simulations were performed, including rapid quenching, slow annealing, and heating, starting from different ordered and random configurations. The simulated system consisted of $12^3/2$ or $24^3/2$ classical spins in an fcc lattice with periodic boundary conditions. The MC algorithm by Walstedt and Walker¹⁶ was employed.

At fields $B < B_c/3$, the continuous degeneracy of the MF structure of Eq. (2) was lifted and the two states $d_2 = 0, d_3^2 = 1 - (3B/B_c)^2$ and $2d_2^2 = 1 - (3B/B_c)^2, d_3 = 0$ were found. The free-energy difference of these structures was calculated by integrating the difference in their magnetizations, $\Delta F(B) = \int_B^{B_c/3} \Delta M(B') dB'$, at 15 nK and $\Delta\lambda/|\lambda_{\min}(1,0,0)| = 0.0004$. The structure with $d_3 \neq 0$ turned out to have a slightly lower free energy. Similarly, the continuous degeneracy of the $\langle 1,0,0 \rangle$ structures at $B > B_c/3$ was lifted and a 3-k state was stabilized, in agreement with our previous studies.^{8,12}

In order to compare measured and theoretical magnetic structure factors, one should know how close to thermal equilibrium the system develops during the experiment. The observed time-dependent effects^{1,2,17} indicate that the time scale of the ordering is on the order of seconds. Therefore, domains of structures with free energies slightly higher than that of the equilibrium configuration may be present. The problem of metastability particularly concerns the $\langle 1,0,0 \rangle$ order, for which the degeneracy in the limit $\Delta\lambda \rightarrow 0_+$ is lifted only by thermal fluctuations. One can expect that the value of the observed $\langle 1,0,0 \rangle$ magnetic structure factor is between the limits given by the thermodynamical equilibrium state and a mixture of domains with equal overall $\langle 1,0,0 \rangle$ structure factors.

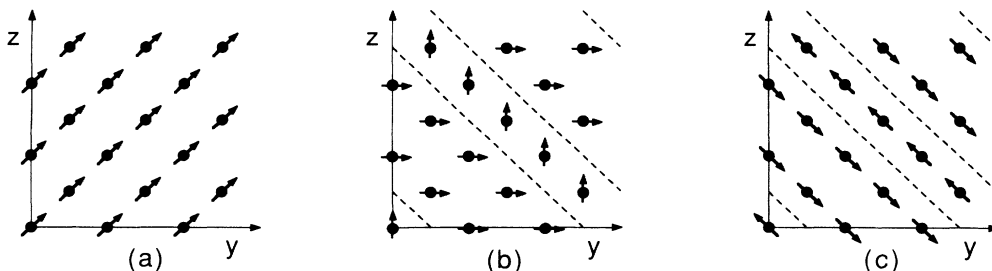


FIG. 1. The spin structures of copper for $[01\bar{1}]$ alignment of the magnetic field, as given by Eq. (2) for $d_3 = 0$. (a) $B = 0$: antiferromagnetic $\mathbf{Q} = (1,0,0)$ structure consisting of alternating ferromagnetic planes. (b) $0 < B < B_c/3$: structure with ordering vectors $(1,0,0)$ and $\pm(0, \frac{2}{3}, \frac{2}{3})$, illustrated at $B = 0.17B_c$. (c) $B = B_c/3$: structure with $\pm(0, \frac{2}{3}, \frac{2}{3})$.

Figure 2(a) shows the calculated contour diagrams of $|\mathbf{S}(0, \frac{2}{3}, \frac{2}{3})|^2$ and the averaged $\langle 1,0,0 \rangle$ structure factor $\frac{1}{3} \{ |\mathbf{S}(1,0,0)|^2 + |\mathbf{S}(0,1,0)|^2 + |\mathbf{S}(0,0,1)|^2 \}$ in the plane of T and B . These results were produced by heating the spin system at sixteen equidistant values of magnetic field between 0 and 0.30 mT, performing 500 MC steps per spin with intervals of 2 nK. The stable structures described above were chosen as the initial configurations. The resemblance to the experimental phase diagram¹ of Fig. 2(b) is striking. A detailed comparison is, however, difficult because the temperature was not measured in the experiment; instead, the data are shown as a function of the warm-up time t . Particularly, T at $t=0$ and the warm-up rate dT/dt are unknown. The heat input via spin-lattice relaxation as well as the specific heat are ex-

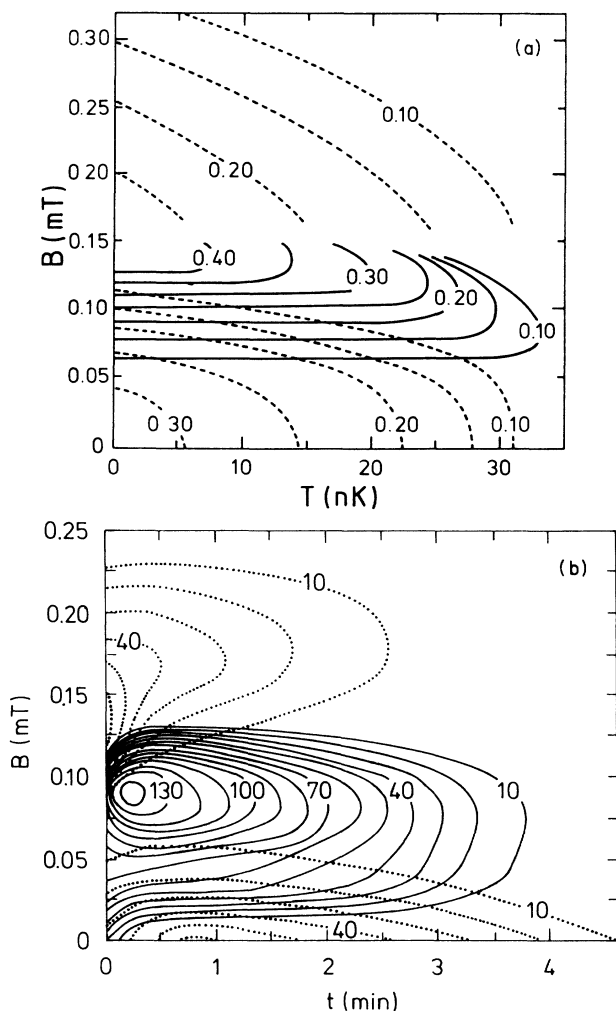


FIG. 2. (a) Contour diagrams of the magnetic structure factor $|\mathbf{S}(0, \frac{2}{3}, \frac{2}{3})|^2$ (solid lines) and the averaged $\langle 1,0,0 \rangle$ structure factor (dashed lines), obtained from MC heating runs for $\Delta\lambda/|\lambda_{\min}(1,0,0)| = 0.0018$. (b) The measured (Ref. 1) neutron-intensity contour diagram of the $(0, \frac{2}{3}, \frac{2}{3})$ (solid lines) and the $(1,0,0)$ (dotted lines) Bragg reflections as functions of the external magnetic field and time after the end of adiabatic demagnetization to various fields. Temperature increases with time. The neutron intensities are proportional to $|\mathbf{S}(0, \frac{2}{3}, \frac{2}{3})|^2$ and $|\mathbf{S}(1,0,0)|^2$, respectively.

pected to have a considerable field dependence.

The above analysis concentrates on permanent structures which describe the ground state. In our MC simulations we have also found nonpermanent $\langle 0, \frac{2}{3}, \frac{2}{3} \rangle$ spin arrangements, which are metastable at low temperatures, but may be stabilized close to T_c . In addition, they can play an important role in the observed^{1,2,17} kinetics of the ordering.

For the region of fields $0.10 \text{ mT} < B < 0.18 \text{ mT}$, a nonpermanent 4- \mathbf{k} state with $\pm (\frac{2}{3}, \frac{2}{3}, 0)$ and $\pm (\frac{2}{3}, -\frac{2}{3}, 0)$ order was obtained. In a numerical MF calculation, we found it to be stable near T_c . This explains the relatively fast decay of the measured $(1,0,0)$ neutron reflection at high fields and the gap between the $(1,0,0)$ and $(0, \frac{2}{3}, \frac{2}{3})$ neutron-intensity contours around 0.13 mT; see Fig. 2(b).

In simulations at $B > 0.18 \text{ mT}$, no metastable states were found. At $B < 0.10 \text{ mT}$, in addition to the permanent structure of Eq. (2), nonpermanent 6- \mathbf{k} and 12- \mathbf{k} structures with only $\langle 0, \frac{2}{3}, \frac{2}{3} \rangle$ order were obtained. The several metastable states at low fields could explain why the measured neutron reflection increases more slowly than at high fields; see Fig. 2(b).

Finally, we describe the calculated spin structures for the magnetic field in the $[001]$ direction. This case is relevant for understanding the measured field-entropy phase diagram.¹⁵ In agreement with the experiment, we find three antiferromagnetic phases as a function of the field. In the low-field phase, illustrated in Fig. 3(a), the $\pm (0, \frac{2}{3}, \frac{2}{3})$ and $\pm (0, \frac{2}{3}, -\frac{2}{3})$ modulations are singled out with equal amplitudes. The phase in intermediate fields is modulated either by the vectors $\pm (0, \frac{2}{3}, \frac{2}{3})$ or $\pm (0, \frac{2}{3}, -\frac{2}{3})$; see Fig. 3(b). These structures also have

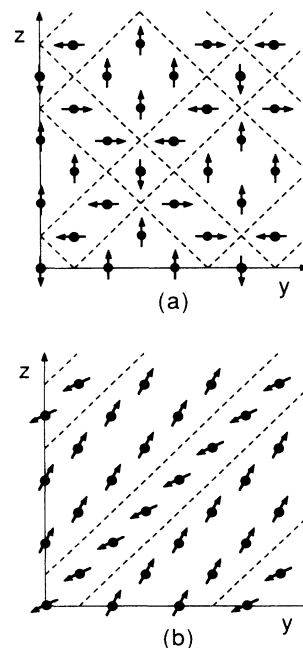


FIG. 3. Spin structures in the $[001]$ alignment of the magnetic field. The $\pm (0, \frac{2}{3}, \frac{2}{3})$ and $\pm (0, \frac{2}{3}, -\frac{2}{3})$ order is in the yz plane while the $(0,0,1)$ order points out of the plane. (a) $B < B_c/3$. (b) $B_c/3 < B < B_c/\sqrt{5}$.

degenerate $\langle 1,0,0 \rangle$ order. The high-field state shows $\langle 1,0,0 \rangle$ modulation only. The theoretical critical fields $B_c/3 \approx 0.13$ mT and $B_c/\sqrt{5} \approx 0.18$ mT for transitions between the ordered phases coincide closely with the measured values 0.12 and 0.17 mT, respectively. The transitions are of first order as observed.¹⁵

Our theory of coexisting $\langle 0, \frac{2}{3}, \frac{2}{3} \rangle$ and $\langle 1,0,0 \rangle$ order in copper can be widely generalized: The essential features are the double-well structure of the potential and the differing anisotropy properties associated with the two minima. When applied, in particular, to antiferromagnetic order of period three, we find that it can coexist with either ferromagnetism or with antiferromagnetism of period two or four. $\text{USb}_{0.9}\text{Te}_{0.1}$ with coexisting ferromagnetic and multiaxial antiferromagnetic order provides an example.¹⁸ We also expect that our ideas will enlighten the coexistence of ferromagnetism and the types-I and -II antiferromagnetism observed in NiS_2 .¹⁹

In conclusion, the magnetic phase diagram of nuclear spins in copper has been investigated theoretically with considerable success. In this fcc system, the strongly anisotropic spin interactions stabilize the external-field-induced $\langle 0, \frac{2}{3}, \frac{2}{3} \rangle$ order, while the zero-field and high-field structures are of $\langle 1,0,0 \rangle$ -type. The spin structure at low fields displays both $\langle 0, \frac{2}{3}, \frac{2}{3} \rangle$ and $\langle 1,0,0 \rangle$ order, unlike any previously found magnetic structure. Our results explain the observations on copper: the recent neutron-diffraction experiments^{1,2} as well as the measured field-entropy phase diagram.¹⁵ Nuclear spins in copper indeed provide an

ideal system to study magnetism starting from first principles.

Note added in proof

In the limit $\Delta\lambda \rightarrow 0_+$, it was possible to determine the MF ground state analytically; qualitatively similar results are obtained numerically for $0 < \Delta\lambda < 0.01 |\lambda_{\min}(1,0,0)|$. For $\Delta\lambda$ outside this region, fluctuations beyond the MF theory would be needed to explain the observed^{1,2} antiferromagnetic neutron reflections. Our MF solution contains the relevant physics in this case as well in the sense that it gives the field regions in which the strongly field-dependent energy differences between the states are small enough for fluctuations to overcome.

An application of external magnetic field lifts the degeneracy of the 12 cubic-symmetry-related $\langle 0, \frac{2}{3}, \frac{2}{3} \rangle$ modulations. Our results explain the selection of the ordering vectors in the $[01\bar{1}]$ field direction that was used in the neutron diffraction experiments.¹ More recent measurements [A. J. Annala *et al.* (unpublished)] have verified our selection rules for the field direction $[001]$, discussed above, as well as those for the $[111]$ direction, obtained by extending the present analysis.

We thank K. N. Clausen, P.-A. Lindgård, O. V. Lounasmaa, D. J. Miller, R. M. Nieminen, and M. M. Salomaa for valuable discussions. This work has been supported by the Academy of Finland. H.E.V. acknowledges support by the Magnus Ehrnrooth Foundation.

¹A. J. Annala, K. N. Clausen, P.-A. Lindgård, O. V. Lounasmaa, A. S. Oja, K. Siemensmeyer, M. Steiner, J. T. Tuoriniemi, and H. Weinfurter, *Phys. Rev. Lett.* **64**, 1421 (1990).

²T. A. Jyrkkiö, M. T. Huiku, O. V. Lounasmaa, K. Siemensmeyer, K. Kakurai, M. Steiner, K. N. Clausen, and J. K. Kjems, *Phys. Rev. Lett.* **60**, 2418 (1988).

³P. J. Brown, *Physica (Amsterdam)* **137B**, 31 (1986), and references therein. An extensive study of the very different fcc antiferromagnetism of cerium monopnictides can be found in J. M. Wills and B. R. Cooper, *Phys. Rev. B* **36**, 3809 (1987), and in references therein.

⁴L. H. Kjaldman and J. Kurkijärvi, *Phys. Lett.* **71A**, 454 (1979).

⁵P. Kumar, J. Kurkijärvi, and A. S. Oja, *Phys. Rev. B* **33**, 444 (1986).

⁶P.-A. Lindgård, X.-W. Wang, and B. N. Harmon, *J. Magn. Mater.* **54-57**, 1052 (1986).

⁷S. J. Frisken and D. J. Miller, *Phys. Rev. Lett.* **57**, 2971 (1986); *Phys. Rev. B* **37**, 10884 (1988).

⁸H. E. Vieriö and A. S. Oja, *Phys. Rev. B* **36**, 3805 (1987).

⁹P.-A. Lindgård, *Phys. Rev. Lett.* **61**, 629 (1988).

¹⁰P.-A. Lindgård, *J. Phys. (Paris)*, Colloq. **49**, C8-2051 (1988).

¹¹S. J. Frisken and D. J. Miller, *Phys. Rev. Lett.* **61**, 1017 (1988).

¹²H. E. Vieriö and A. S. Oja, in *Quantum Fluids and Solids — 1989*, edited by G. G. Ihas and Y. Takano, AIP Conference Proceedings No. 194 (American Institute of Physics, New York, 1989), p. 305.

¹³A. S. Oja, X.-W. Wang, and B. N. Harmon, *Phys. Rev. B* **39**, 4009 (1989).

¹⁴J. Villain, *J. Phys. Chem. Solids* **11**, 303 (1959); A. Abragam and M. Goldman, *Nuclear Magnetism: Order and Disorder* (Clarendon, Oxford, 1982).

¹⁵M. T. Huiku, T. A. Jyrkkiö, J. M. Kyynäräinen, A. S. Oja, and O. V. Lounasmaa, *Phys. Rev. Lett.* **53**, 1692 (1984).

¹⁶R. E. Walstedt and L. R. Walker, *J. Appl. Phys.* **53**, 7985 (1982).

¹⁷K. Siemensmeyer, K. Kakurai, M. Steiner, T. A. Jyrkkiö, M. T. Huiku, and K. N. Clausen, *J. Appl. Phys.* **67**, 5433 (1990).

¹⁸J. Rossat-Mignod, P. Burlet, O. Vogt, and G. H. Lander, *J. Phys. C* **12**, 1101 (1979).

¹⁹J. M. Hastings and L. M. Corliss, *IBM J. Res. Dev.* **14**, 227 (1970). For more recent work on NiS_2 see T. Miyadai, K. Kikuchi, and H. Ito, *Phys. Lett.* **67A**, 61 (1978).